



Climate velocity reveals increasing exposure of deep-ocean biodiversity to future warming

Isaac Brito-Morales^{ID 1,2}✉, David S. Schoeman^{ID 3,4}, Jorge García Molinos^{ID 5,6,7}, Michael T. Burrows^{ID 8}, Carissa J. Klein¹, Nur Arafah-Dalmau^{ID 1,9}, Kristin Kaschner¹⁰, Cristina Garilao¹¹, Kathleen Kesner-Reyes¹² and Anthony J. Richardson^{2,13}

Slower warming in the deep ocean encourages a perception that its biodiversity is less exposed to climate change than that of surface waters. We challenge this notion by analysing climate velocity, which provides expectations for species' range shifts. We find that contemporary (1955–2005) climate velocities are faster in the deep ocean than at the surface. Moreover, projected climate velocities in the future (2050–2100) are faster for all depth layers, except at the surface, under the most aggressive GHG mitigation pathway considered (representative concentration pathway, RCP 2.6). This suggests that while mitigation could limit climate change threats for surface biodiversity, deep-ocean biodiversity faces an unavoidable escalation in climate velocities, most prominently in the mesopelagic (200–1,000 m). To optimize opportunities for climate adaptation among deep-ocean communities, future open-ocean protected areas must be designed to retain species moving at different speeds at different depths under climate change while managing non-climate threats, such as fishing and mining.

Climate change drives the reorganization of ecosystems, with most species moving poleward but at different rates, and others moving in different directions or not at all^{1,2}. These changes are affecting the ecosystem goods and services delivered by biodiversity, from primary production³ to fisheries yield⁴. In marine systems, knowledge of the spatial reorganization of biodiversity comes largely from the upper 200 m of the ocean, where much of the biodiversity resides⁵ and is well-studied. There is far less information about how biodiversity below the surface ocean—including the vast communities of myctophids (the most abundant fish in the world⁶) and the unique species associated with seamounts, canyons and seeps⁷—might respond to climate change⁸. Because the rate of warming has been fastest at the surface⁹ and declines with depth¹⁰, there is a perception that the deep ocean could be spared the worst impacts of climate change.

The paucity of data for all but the most common or prominent marine taxa means that we must often rely on proxy metrics when assessing threats of climate change. Here, we use such a proxy, horizontal climate velocity^{11,12}, to explore expectations for species' range shifts under projected future ocean warming. This metric estimates the speed and direction of isotherm displacement under a changing climate, providing a simple and generic metric of exposure to warming that predicts species' range shifts^{13,14}, especially for those with conservative thermal niches¹⁵. An alternative response to ocean warming is vertical shifts in species' distributions. These can be important within depth zones defined by species' environmental requirements¹⁶ but mainly in areas with particularly steep vertical

temperature gradients¹⁷. We do not consider vertical climate velocities here because we investigate the open ocean across coarse depth layers within which vertical temperature responses might operate (see Methods).

Using data from Coupled Model Intercomparison Project Phase 5 (CMIP5) climate models averaged annually and re-gridded to 1° resolution by bilinear interpolation, we estimated climate velocity¹² as the temporal rate of change of temperature over the corresponding spatial gradient (see Methods). Climate velocity was calculated for the contemporary climate (1955–2005; historical model runs) and for three future (2050–2100) climate scenarios generated under three of the IPCC representative concentration pathways (RCPs)¹⁸. The first RCP has emissions peaking by 2020 and declining thereafter (RCP 2.6), the second has emissions peaking by 2040 (RCP 4.5) and the final scenario has emissions continuing to rise throughout the twenty-first century (RCP 8.5). We analysed climate velocities (averaged by volume) in four depth layers: surface (0–200 m), mesopelagic (200–1,000 m), bathypelagic (1,000–4,000 m) and abyssopelagic (>4,000 m)¹⁹. Using the same model outputs for all analyses (historical and future), ensures that any biases caused by data collection or processing propagate equally across all outputs. To evaluate how marine species are exposed to contemporary climate velocity, we combined previous estimates of climate velocity with AquaMaps data, the most comprehensive data available for the distribution of marine biodiversity²⁰ (20,019 species; see Methods). This dataset comprises a range of vertebrates (for example, fish, birds, mammals and reptiles), invertebrates (for example, molluscs, arthropods

¹School of Earth and Environmental Sciences, The University of Queensland, St Lucia, Queensland, Australia. ²Commonwealth Scientific and Industrial Research Organisation (CSIRO) Oceans and Atmosphere, BioSciences Precinct (QBP), St Lucia, Queensland, Australia. ³Global-Change Ecology Research Group, School of Science and Engineering, University of the Sunshine Coast, Maroochydore, Queensland, Australia. ⁴Centre for African Conservation Ecology, Department of Zoology, Nelson Mandela University, Port Elizabeth, South Africa. ⁵Arctic Research Center, Hokkaido University, Sapporo, Japan. ⁶Global Station for Arctic Research, Global Institution for Collaborative Research and Education, Hokkaido University, Sapporo, Japan. ⁷School of Environmental Science, Hokkaido University, Sapporo, Japan. ⁸Scottish Association for Marine Science, Oban, UK. ⁹Centre for Biodiversity and Conservation Science, School of Biological Sciences, The University of Queensland, St Lucia, Queensland, Australia. ¹⁰Department of Biometry and Environmental Systems Analysis, Albert-Ludwigs University, Freiburg im Breisgau, Germany. ¹¹GEOMAR, Helmholtz-Zentrum für Ozeanforschung, Kiel, Germany. ¹²Quantitative Aquatics, International Rice Research Institute, Los Baños, Philippines. ¹³Centre for Applications in Natural Resource Mathematics, School of Mathematics and Physics, The University of Queensland, St Lucia, Queensland, Australia. ✉e-mail: i.britomorales@uq.edu.au

Table 1 | Global climate velocity (km per decade) medians (cell area-weighted) from an ensemble-average of 11 CMIP5 models (uncertainty illustrated by 25th and 75th percentiles)

Ocean layer	Contemporary climate (1955–2005)	RCP 2.6 (2050–2100)	RCP 4.5 (2050–2100)	RCP 8.5 (2050–2100)
Surface (0–200 m)	12.28 (7.02, 21.78)	6.03 (0.67, 14.80) [0.5]	25.64 (15.36, 48.90) [2.1]	85.55 (56.22, 158.97) [7.0]
Mesopelagic (200–1,000 m)	6.28 (-0.62, 15.06)	49.92 (16.19, 113.83) [7.0]	85.23 (31.70, 179.03) [13.5]	135.33 (60.11, 292.25) [21.5]
Bathypelagic (1,000–4,000 m)	24.64 (7.89, 42.61)	76.47 (21.67, 134.28) [3.1]	90.56 (26.35, 147.62) [3.7]	114.02 (35.16, 177.05) [4.6]
Abyssopelagic (>4,000 m)	43.14 (38.38, 59.48)	67.98 (47.60, 109.23) [1.6]	74.91 (51.37, 113.24) [1.7]	78.05 (54.19, 116.48) [1.8]

For each future depth-emission scenario combination, the relative increase in climate velocity from the contemporary climate is given in square brackets.

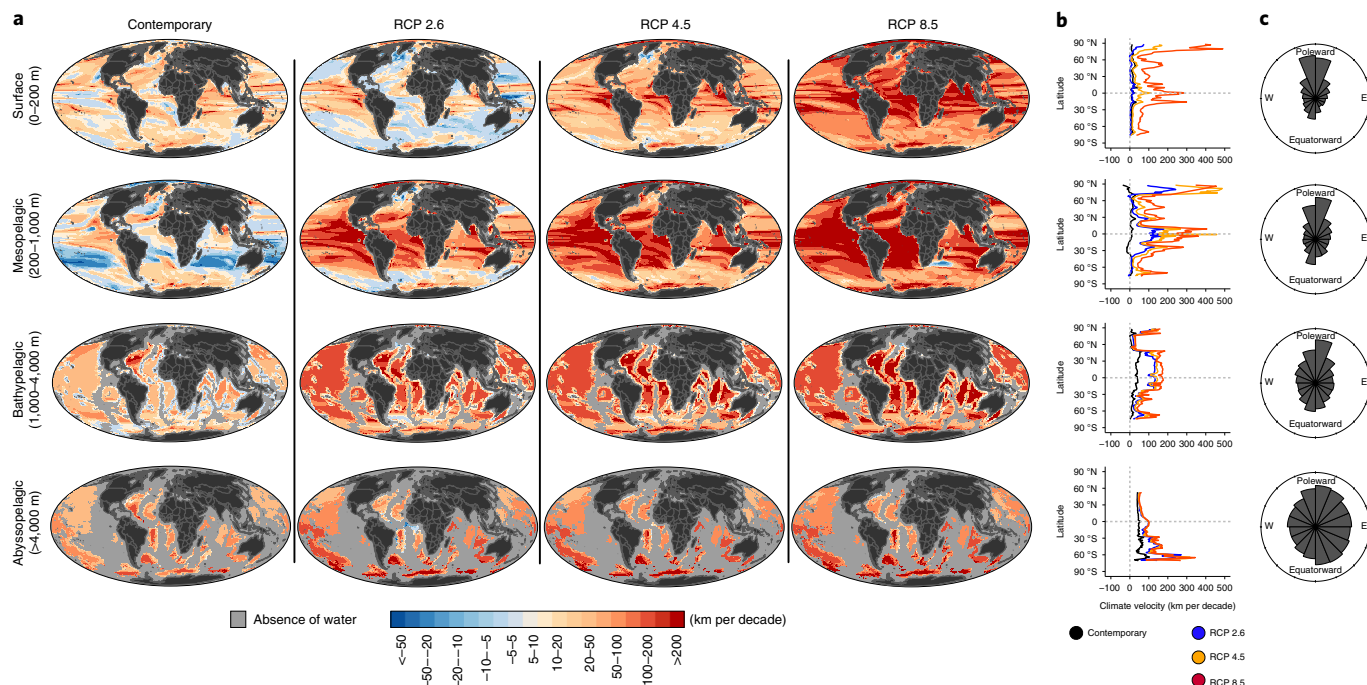


Fig. 1 | Climate velocity (km per decade) in the global ocean. **a**, Contemporary (1955–2005) and projected future sea temperatures (2050–2100) at four different depths under three IPCC emission scenarios (RCP2.6, RCP4.5 and RCP8.5). Grey grid squares in deeper layers represent areas with no corresponding sea temperature data available because of seafloor features extending toward the surface. **b**, Latitudinal plots representing median magnitudes of climate velocity by 1° of latitude. **c**, Directional roses representing the relative frequency of direction of climate velocity for the contemporary period (1955–2005); we have illustrated the directions only for contemporary climate velocity here because those for all emission scenarios are almost identical (see Extended Data Fig. 3).

and corals) and macroalgae (green, red and brown; Supplementary Table 3). We further explored the consequences of our results by intersecting data on climate velocity and biodiversity within the current global network of large marine protected areas (MPAs).

The magnitude of contemporary climate velocity is relatively fast in the surface layer, slower in the mesopelagic layer, but becomes fastest in the bathypelagic and abyssopelagic layers (Table 1 and Fig. 1). This contrasting pattern with depth arises because the rate of warming (the numerator of climate velocity) is presently greatest at the surface and declines with depth but the spatial gradient (the denominator of climate velocity) becomes gentler (flatter) with depth (see Extended Data Fig. 1 and Supplementary Table 1). The relative magnitude of these contrasting patterns leads to the rapid velocities in the bathypelagic and abyssopelagic layers (henceforth the deep ocean). Fast climate velocities in the deep ocean suggest

that species there are currently at least as exposed to effects of warming, in terms of distribution shift²¹, as species in the surface ocean and could therefore be at similar risk of extirpation²². This provides strong motivation to consider future impacts of ocean warming in this under-explored habitat²².

Projected future climate velocities increase for each depth layer and future scenario, except at the surface for RCP 2.6. This pathway of aggressive GHG mitigation from 2020 until the end of the century (Table 1 and Fig. 1) leads to cooling and thus slower climate velocities at the surface. However, the prognosis is not as optimistic for deeper layers under RCP 2.6, with climate velocities in the mesopelagic layer increasing sevenfold to rates more than four times those currently experienced at the surface. Climate velocity in the abyssopelagic layer also increases, reaching 5.5 times the rates currently experienced at the surface. Therefore, moderating surface warming

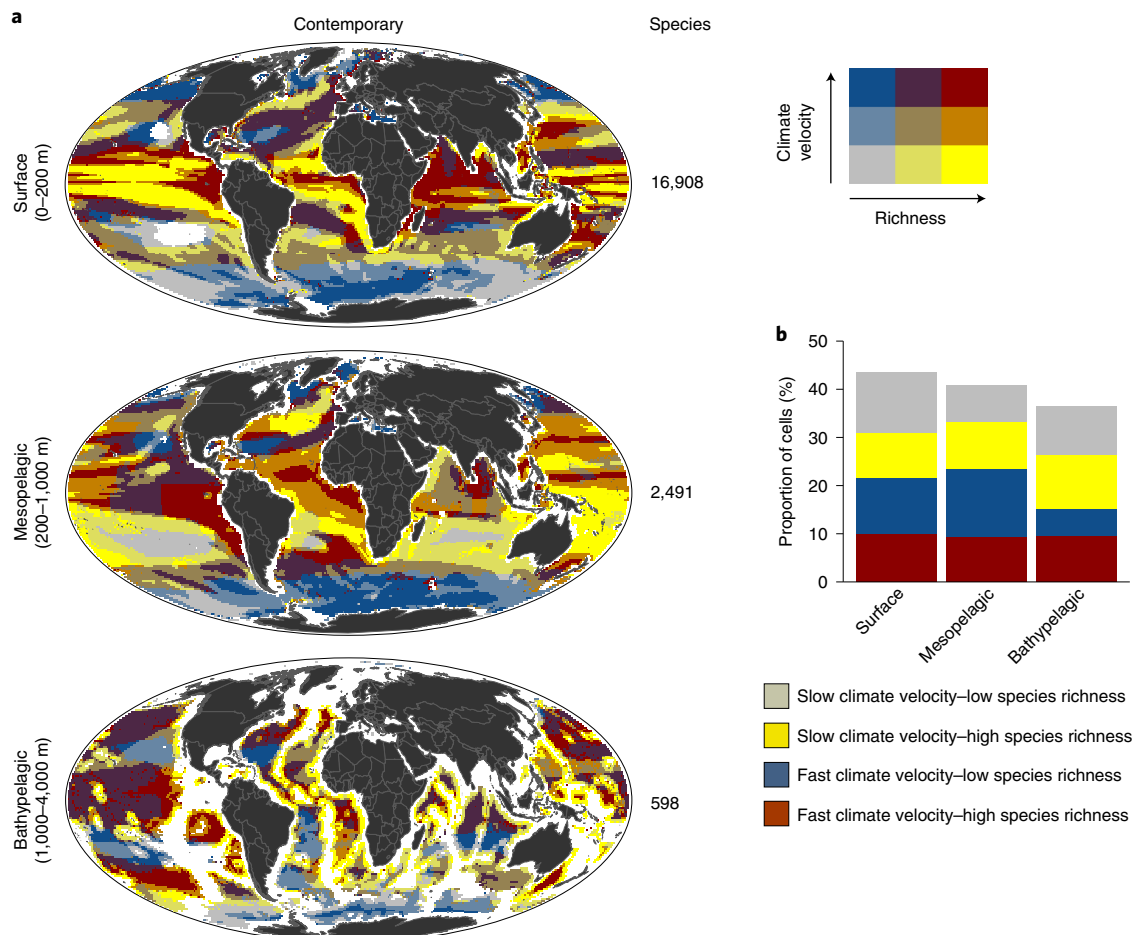


Fig. 2 | The relationship between contemporary climate velocity and marine biodiversity. **a**, Bivariate choropleth maps overlapping the magnitude of climate velocity with species' richness at three depth zones in the ocean. Cells for each depth layer and variable (climate velocity and species' richness) were split into terciles to define categories. Biodiversity within each depth layer has been rescaled relative to its appropriate depth. White grid squares represent areas with no corresponding temperature data available because of seafloor features extending toward the surface. **b**, Proportions of cells (%) for the four categories representing the most extreme overlapping terciles for the relationship between climate velocity and species' richness.

under RCP 2.6 will probably mean that the large-scale redistribution of marine life currently underway in the surface layer^{1,14} might be curtailed but that dramatic distribution changes are likely for biodiversity in the deep ocean²¹.

Under RCP4.5 and RCP 8.5, ongoing surface warming and the continued redistribution of this heat energy through the water column²³ means faster future climate velocities at all depths. Although deep layers will continue to warm more slowly than surface waters (Extended Data Figs. 1 and 4), this process is not projected to alter spatial temperature gradients (Extended Data Fig. 2 and Supplementary Table 1). The result is that future climate velocities across each ocean layer are projected to be faster under RCP4.5 and RCP 8.5 than they are today. Under RCP8.5, future climate velocity in the mesopelagic layer is projected to be >20 times faster than its current value and 11 times faster than contemporary surface climate velocities (Table 1). Importantly, below the mesopelagic layer, estimates of future climate velocity are relatively unaffected by GHG concentration pathway (including RCP2.6), emphasizing the climate change exposure associated with committed warming in the deep ocean resulting from downmixing of heat that has already been taken up at the surface. Although mitigation measures aiming to reduce GHG emissions would be expected to be effective in terms of alleviating climate change exposure in surface waters of the global ocean by 2100, they would achieve limited benefits at greater depths.

Comparing the spatial distribution of contemporary climate change exposure, as measured by the magnitude of climate velocity, with that of species' richness highlights potential areas of risk and of climate refuge at different depths (Fig. 2) both of which are relevant for marine conservation. For instance, 10% of surface waters experience overlapping areas of fast climate velocity and high species' richness (Fig. 2a). These exposed areas are mainly in tropical and subtropical latitudes (Fig. 2a mid-south Atlantic and central Pacific Ocean), with some striking exceptions in temperate latitudes. The mesopelagic layer exhibits similar congruency between biodiversity and climate change exposure (9% of cells) but with slightly more climate refugia in biodiverse areas (14% of cells with slow climate velocity and high species' richness) than surface waters (12% of cells) (Fig. 2b). The pattern for the bathypelagic layer reveals areas of high biodiversity exposed to climate change widespread across all latitudes, except for polar regions (Fig. 2c). That many of those threatened regions are in areas beyond national jurisdiction²⁴ not only highlights challenges associated with climate change and conservation but also the need for international cooperation in addressing this problem.

Taken together, these results describe a rapid acceleration of climate change exposure throughout the water column by the second half of the twenty-first century. Because deep-sea species are physiologically adapted to relatively stable temperatures characteristic of

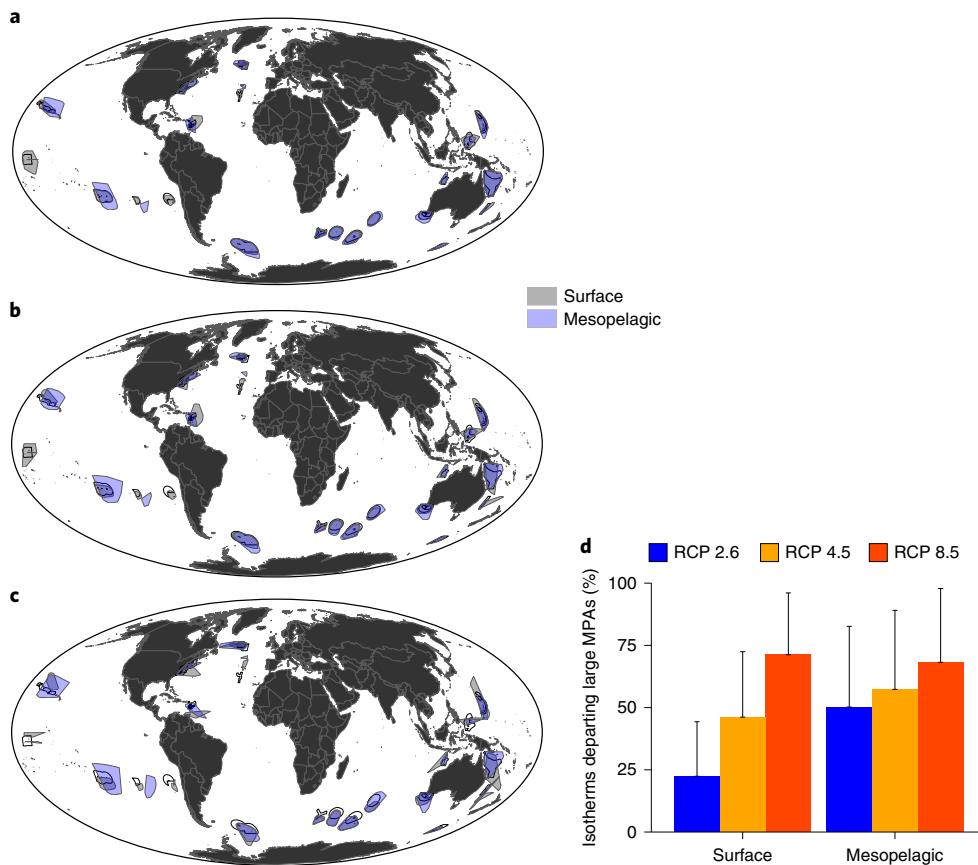


Fig. 3 | Future distribution of thermal habitat presently within large ($>100,000 \text{ km}^2$) MPAs. **a-c**, Projected MPA thermal habitats under RCP 2.6 (a), RCP 4.5 (b) and RCP 8.5 (c). Coloured polygons represent convex hulls surrounding the ending positions of isotherms projected forward in time³⁶ from 2019 to 2100. **d**, Average proportion of isotherms departing each large MPA ($n=23 \pm \text{s.d.}$) by 2100 at the ocean surface and in the mesopelagic under three emission scenarios (RCP 2.6, RCP 4.5 and RCP 8.5).

waters below the surface layer²⁵, they are considered vulnerable to even small temperature increases in the absence of nearby thermal refugia^{21,26}. Implications for deep-sea biodiversity, which remains poorly studied, could therefore be worse than those currently observed for species in the surface ocean, even under optimistic future scenarios (Fig. 2).

Fastest climate velocities and largest differences relative to current conditions are projected for the mesopelagic layer under all emission scenarios, which is cause for particular concern. This layer is inhabited by small mesopelagic fish⁵ such as those from the genus *Cyclothona*, probably the most abundant vertebrate in the world. The huge biomass of mesopelagic fish not only supports commercial tuna and squid fisheries but it also drives the vertical flux of matter in the deep ocean²⁷ as the fish migrate from surface feeding layers during the night to deeper layers during the day, where they release carbon and nitrogen through respiration and excretion⁶. How the trophic connectivity to commercial fish stocks and the vertical connectivity of carbon transfer to the deep ocean will be affected by the probable rearrangement of mesopelagic ecosystems remains an open question.

Faster climate velocities at depth in the future could mean that unique seamount and canyon communities move downslope to find cooler refugia from warming, mirroring the tendency of terrestrial plants and animals to move to greater altitude with warming²⁸. Those deep-ocean species limited by pressure, however, would need to either adapt or move between distant habitats¹⁶, in ways similar to those exhibited by high-altitude communities on land that need to move between mountaintops because of climate change. In the

bathypelagic and abyssopelagic ocean, the growing threat of warming for biodiversity (Fig. 2) could have a more severe effect on resident species, especially when coupled with declines in pH, oxygen concentration and flux of organic matter. For instance, warming could induce formation and precipitation to the seafloor of methane crystals at deep margins²⁹. This process could disrupt microorganisms that oxidize methane and could also promote range expansions of cold-seep biodiversity²¹.

Not only does the speed of climate velocity vary with depth but so does its direction (Fig. 1c), regardless of future scenario (Extended Data Fig. 3). In the surface layer, climate velocities are mostly poleward but this dominant direction declines progressively in importance with depth, a pattern consistent across all scenarios. For species tracking their shifting thermal niches in response to warming, these changes in direction of climate velocity might produce range mismatches among species across depths. This could compromise the vertical connectivity in the deep ocean that underpins mesopelagic and bathypelagic food webs⁶. Moreover, the potential spatial reorganization and decoupling of vertical connectivity among thermal niches could compromise the sustainable management of mesopelagic fish resources. Altered vertical connectivity of thermal niches could also superimpose an additional threat on bathypelagic and abyssopelagic biodiversity, already increasingly threatened by fishing and mining^{4,27,30}. For example, there is increasing interest in exploiting mesopelagic myctophids⁶, while, on the seafloor of the deep ocean, more mining licences are being allocated for future extraction purposes²⁴. Finally, as climate velocity becomes multidirectional with depth (Fig. 1c and Extended

Data Fig. 3), the expectation of species' range shifts in response to warming will depend, in part, on the match or mismatch between directions of climate velocity vectors and those of ocean currents³¹. This could compromise the ability of species to populate potentially available thermal niches so that consideration of ocean currents will also be relevant in identifying priority areas for conservation³².

The committed future exposure of the deep ocean to warming provides strong motivation for exploring adaptation options that might increase the resilience of its ecosystems across all depth layers³³. The proclamation of large, no-take MPAs has accelerated in recent decades³⁴ and has the benefit of providing marine species with increased opportunity to adapt to changing climate³⁵. But the often-contrasting directions of climate velocity at different depths pose challenges not so far considered in marine conservation planning. To illustrate the associated complexity, we constructed climate velocity trajectories^{14,36} for thermal conditions presently within two ocean layers (surface and mesopelagic) for a selection of established large MPAs (>100,000 km² in extent) over the period 2019–2100 (see Methods). Isotherms in the surface and mesopelagic layers often move beyond existing MPA boundaries at different speeds and in contrasting directions, depending on emissions scenario (Fig. 3a–c and Extended Data Fig. 3). Importantly, MPAs tend to retain more of their thermal habitat under RCP 2.6 for both depths but especially in the surface layer, and progressively less under RCP 4.5 and RCP 8.5 (Fig. 3d). Intersecting the current biodiversity within large MPAs also highlights the different levels of climate change exposure that current biodiversity will potentially face at different depths in the ocean (Extended Data Fig. 5). For instance, the highest proportions of species that will be exposed to novel climate regimes within large MPAs will be mainly in the mesopelagic and bathypelagic layers and less at the surface. Limiting emissions (RCP 2.6) could thus be important for retaining species within MPA boundaries, at least at the surface.

Anticipating effects of climate change is an increasingly vital consideration in marine conservation and should be a central theme in ongoing efforts to develop global MPA networks³⁷. However, MPAs are worth the investment only where they can feasibly mitigate present or future threats, such as harvesting, resource extraction or environmental degradation. Where this is the case, several conservation strategies that accommodate a changing climate have been proposed, including: (1) shifting MPAs^{30,38} that adjust their boundaries as biodiversity responds to warming; (2) placing MPAs along future spatial pathways, acting as stepping stones for biodiversity^{36,39}; and (3) including climate-stable areas, such as climate refugia, in MPA networks^{32,36}. However, the complexities of considering the widely different magnitudes and directions of climatic changes at different depths poses a challenge to designing climate-safe MPAs in the open ocean³².

The fact that uncertainty among CMIP5 models in climate velocity estimates increases with depth (see Caveat section in Methods) highlights limitations of present-generation climate models and this will require more attention in future studies. Emerging CMIP6 models, which are increasingly reliable, might improve temperature estimates at depth. But how climate change could differentially affect biodiversity at different depths in the ocean—and how we might design robust, climate-resilient protected areas to conserve this biodiversity—will remain an enduring challenge, irrespective of how well we estimate climate change impacts in the deep ocean.

As society contemplates a potential future that involves decades of accelerating climate change, impacts on biodiversity below the ocean surface should not be ignored. To afford deep-sea biodiversity the best possible opportunity to adapt to the unavoidable escalation of exposure to climate threats, the Precautionary Principle suggests that limits should be placed on exploitation of deep-ocean resources by fishing fleets and by mining, hydrocarbon and other extractive activities. The most obvious way to achieve this outcome

is to now plan networks of large MPAs for the deeper ocean that would exclude or limit extractive human uses, and to identify and protect potential refuge areas, such as slopes and complex bathymetric features, that might hold distinct climatic conditions and retain species.

Online content

Any methods, additional references, Nature Research reporting summaries, source data, extended data, supplementary information, acknowledgements, peer review information; details of author contributions and competing interests; and statements of data and code availability are available at <https://doi.org/10.1038/s41558-020-0773-5>.

Received: 21 June 2019; Accepted: 7 April 2020;

Published online: 25 May 2020

References

1. Poloczanska, E. S. et al. Global imprint of climate change on marine life. *Nat. Clim. Change* **3**, 919–925 (2013).
2. Poloczanska, E. S. et al. Responses of marine organisms to climate change across oceans. *Front. Mar. Sci.* **3**, 62 (2016).
3. Pecl, G. T. et al. Biodiversity redistribution under climate change: impacts on ecosystems and human well-being. *Science* **355**, eaai9214 (2017).
4. Free, C. M. et al. Impacts of historical warming on marine fisheries production. *Science* **363**, 979–983 (2019).
5. Costello, M. J. & Chaudhary, C. Marine biodiversity, biogeography, deep-sea gradients, and conservation. *Curr. Biol.* **27**, R511–R527 (2017).
6. Irigoien, X. et al. Large mesopelagic fishes biomass and trophic efficiency in the open ocean. *Nat. Commun.* **5**, 3271 (2014).
7. Harris, P. T., Macmillan-Lawler, M., Rupp, J. & Baker, E. K. Geomorphology of the oceans. *Mar. Geol.* **352**, 4–24 (2014).
8. Webb, T. J., Berghe, E. V. & O'Dor, R. Biodiversity's big wet secret: the global distribution of marine biological records reveals chronic under-exploration of the deep pelagic ocean. *PLoS ONE* **5**, e10223 (2010).
9. Cheng, L., Abraham, J., Hausfather, Z. & Trenberth, K. E. How fast are the oceans warming? *Science* **363**, 128–129 (2019).
10. Desbruyères, D., McDonagh, E. L., King, B. A. & Thierry, V. Global and full-depth ocean temperature trends during the early twenty-first century from Argo and repeat hydrography. *J. Climate* **30**, 1985–1997 (2016).
11. Loarie, S. R. et al. The velocity of climate change. *Nature* **462**, 1052–1055 (2009).
12. Burrows, M. T. et al. The pace of shifting climate in marine and terrestrial ecosystems. *Science* **334**, 652–655 (2011).
13. Pinsky, M. L., Worm, B., Fogarty, M. J., Sarmiento, J. L. & Levin, S. A. Marine taxa track local climate velocities. *Science* **341**, 1239–1242 (2013).
14. García Molinos, J. et al. Climate velocity and the future global redistribution of marine biodiversity. *Nat. Clim. Change* **6**, 83–88 (2016).
15. Chivers, W. J., Walne, A. W. & Hays, G. C. Mismatch between marine plankton range movements and the velocity of climate change. *Nat. Commun.* **8**, 14434 (2017).
16. Jordà, G. et al. Ocean warming compresses the three-dimensional habitat of marine life. *Nat. Ecol. Evol.* **4**, 109–114 (2020).
17. Burrows, M. T. et al. Ocean community warming responses explained by thermal affinities and temperature gradients. *Nat. Clim. Change* **9**, 959–963 (2019).
18. Moss, R. H. et al. The next generation of scenarios for climate change research and assessment. *Nature* **463**, 747–756 (2010).
19. Sayre, R. et al. A three-dimensional mapping of the ocean based on environmental data. *Oceanography* **30**, 90–103 (2017).
20. Kaschner, K. et al. *AquaMaps: Predicted Range Maps for Aquatic Species* v.10/2019 (Global Biodiversity Information Facility, accessed 2019); <https://www.aquamaps.org/>
21. Levin, L. A. & Bris, N. L. The deep ocean under climate change. *Science* **350**, 766–768 (2015).
22. Wiens, J. J. Climate-related local extinctions are already widespread among plant and animal species. *PLoS Biol.* **14**, e2001104 (2016).
23. Balmaseda, M. A., Trenberth, K. E. & Källén, E. Distinctive climate signals in reanalysis of global ocean heat content. *Geophys. Res. Lett.* **40**, 1754–1759 (2013).
24. Wright, G. et al. Marine spatial planning in areas beyond national jurisdiction. *Mar. Policy* (in the press).
25. Ashford, O. S. et al. Phylogenetic and functional evidence suggests that deep-ocean ecosystems are highly sensitive to environmental change and direct human disturbance. *Proc. R. Soc. B* **285**, 20180923 (2018).

26. Pinsky, M. L., Eikeset, A. M., McCauley, D. J., Payne, J. L. & Sunday, J. M. Greater vulnerability to warming of marine versus terrestrial ectotherms. *Nature* **569**, 108–111 (2019).
27. Hidalgo, M. & Bowman, H. I. Developing the knowledge base needed to sustainably manage mesopelagic resources. *ICES J. Mar. Sci.* **76**, 609–615 (2019).
28. Chen, I.-C., Hill, J. K., Ohlemüller, R., Roy, D. B. & Thomas, C. D. Rapid range shifts of species associated with high levels of climate warming. *Science* **333**, 1024–1026 (2011).
29. Phrampus, B. J., Hornbach, M. J., Ruppel, C. D. & Hart, P. E. Widespread gas hydrate instability on the upper U.S. Beaufort margin. *J. Geophys. Res. Solid Earth* **119**, 8594–8609 (2014).
30. Game, E. T. et al. Pelagic protected areas: the missing dimension in ocean conservation. *Trends Ecol. Evol.* **24**, 360–369 (2009).
31. García Molinos, J., Burrows, M. T. & Poloczanska, E. S. Ocean currents modify the coupling between climate change and biogeographical shifts. *Sci. Rep.* **7**, 1–9 (2017).
32. Brito-Morales, I. et al. Climate velocity can inform conservation in a warming world. *Trends Ecol. Evol.* **33**, 441–457 (2018).
33. Venegas-Li, R., Levin, N., Possingham, H. & Kark, S. 3D spatial conservation prioritisation: accounting for depth in marine environments. *Methods Ecol. Evol.* **9**, 773–784 (2018).
34. Morgan, L., Pike, E. & Moffitt, R. How much of the ocean is protected? *Biodiversity* **19**, 148–151 (2018).
35. Roberts, C. M. et al. Marine reserves can mitigate and promote adaptation to climate change. *Proc. Natl Acad. Sci. USA* **114**, 6167–6175 (2017).
36. Burrows, M. T. et al. Geographical limits to species-range shifts are suggested by climate velocity. *Nature* **507**, 492–495 (2014).
37. Visconti, P. et al. Protected area targets post-2020. *Science* **364**, 239–241 (2019).
38. Maxwell, S. M., Gjerde, K. M., Connors, M. G. & Crowder, L. B. Mobile protected areas for biodiversity on the high seas. *Science* **367**, 252–254 (2020).
39. Fredston-Hermann, A., Gaines, S. D. & Halpern, B. S. Biogeographic constraints to marine conservation in a changing climate. *Ann. NY Acad. Sci.* **1429**, 5–17 (2018).

Publisher's note Springer Nature remains neutral with regard to jurisdictional claims in published maps and institutional affiliations.

© The Author(s), under exclusive licence to Springer Nature Limited 2020

Methods

Data sources and processing. Climate velocity was estimated using contemporary and future temperatures from a multimodel ensemble mean derived from 11 general circulation models (GCMs) from the CMIP5 (Earth System Grid Federation, <https://esgf-node.llnl.gov>; see Supplementary Table 2 for details on the models). For contemporary conditions (1955–2005), we used historical model runs, while for future conditions (2050–2100), we used models under three IPCC RCPs¹⁸: RCP 2.6, RCP 4.5 and RCP 8.5. RCP 2.6 represents a strong mitigation scenario, while RCP 4.5 represents a stabilization scenario in which radiative forcing is stabilized at $\sim 4.5 \text{ W m}^{-2}$ by 2100. This leads to a slow rise of $\sim 1^\circ\text{C}$ in ocean surface temperature relative to 2006 levels. By contrast, RCP 8.5 is a reference scenario, which results in a radiative forcing of $\sim 8.5 \text{ W m}^{-2}$ by 2100, representing an increase in ocean surface temperature of 2.4°C relative to 2006 levels.

For the contemporary period, we have preferred modelled data over observational data for two reasons. First, because local climate velocity requires the estimation of the spatial gradient, all estimates should be based on data with the same native resolution, which is not the situation for observational datasets that have much finer spatial resolution (for example, EN4 dataset) than CMIP5 model outputs. Second, while most of the observational data have been interpolated in their horizontal and vertical components, the assumptions underpinning these calculations differ from those associated with GCMs. Using historical runs of the same GCMs used for future projections ensures that any biases caused by data compilation and processing (for example, spatial re-gridding and computation of volume-adjusted means) propagate equally across all outputs.

Temperature data from CMIP5 models have horizontal (latitude and longitude), temporal (time) and vertical (depth) components. Because the horizontal grid resolution was not homogenous among climate models and this could have an effect on the calculation of climate velocity^{40,41}, we re-gridded each climate model to a uniform 1° spatial grid using an area-weighted bilinear interpolation⁴². For the temporal component, we computed annual means by averaging monthly values for each climate scenario. The vertical grid resolution (depth) was also heterogeneous among climate models (Supplementary Table 2). To maintain consistency among models and to facilitate development of the multimodel ensemble, for each model we extracted depths according to four different ocean layers: surface ($0\text{--}200 \text{ m}$), mesopelagic ($200\text{--}1,000 \text{ m}$), bathypelagic ($1,000\text{--}4,000 \text{ m}$) and abyssopelagic ($>4,000 \text{ m}$)⁴³.

For each depth layer, we calculated a volume-weighted average temperature, with volumes of 1° grid squares in each standard depth layer depending on the characteristics of the corresponding depth layers of the individual model under consideration. To avoid artefacts caused by inconsistent numbers of grid cells available by depth for different models, we followed a conservative approach by including only grid cells common to all models within each depth layer. All computation was undertaken using Climate Data Operators⁴⁴ and R (ref. ⁴⁵).

Climate velocity and its calculation. We analysed horizontal rather than vertical climate velocity. Recent empirical evidence⁴⁷ suggests that depth provides refuge from ocean warming only in areas of steep vertical temperature gradients, where a small shift to cooler depths allows species to persist despite surface warming. Where vertical temperature gradients are less steep, such as where the surface mixed layer penetrates further deeper (at high latitudes) or in the deep ocean ($>500 \text{ m}$), vertical shifts would need to be much greater to avoid climate warming. For most of the ocean, therefore, horizontal climate velocity remains a useful proxy of community-level responses to climate change. This is especially pertinent in our analysis because we integrate across large ocean depth layers within which vertical temperature responses might operate. We thus estimated the local horizontal climate velocity for each 1° grid square, at each ocean depth layer of the multimodel ensemble. The temporal trend (numerator of climate velocity) was calculated as the slope of a linear regression of mean annual temperatures ($^\circ\text{C yr}^{-1}$) for the corresponding climate scenario time period. The spatial gradient (denominator of climate velocity) was calculated from the vector sum of the latitudinal and longitudinal pairwise differences of the mean temperature across the corresponding climate scenario time period at each focal cell using a 3×3 neighbourhood window ($^\circ\text{C km}^{-1}$)^{12,36}. We calculated climate velocity based on temperature alone because it is one of the strongest environmental drivers of biodiversity in the ocean^{7,46,47}, is correlated with nutrient availability⁴⁸, has a unimodal relationship with biological performance⁴⁹ and is a key variable impacted by climate change⁴⁹. We chose a climate velocity gradient approach instead of a climate-analogue approach because the local gradient approach is more meaningful for coarse-resolution global analyses³² and preferable when a single variable (here, sea temperature) is used³². All calculations were performed using the VoCC R package⁵⁰.

We use horizontal climate velocity for discrete depth layers in the global ocean, rather than vertical or fully three-dimensional climate velocities, because our expectation is that if realized distributions of marine ectotherms follow thermal tolerance limits⁵¹ but are constrained by fixed depth limits⁵², species' ranges will expand at their leading (cool, poleward) edges at the depth-specific climate velocity of the shallow limit of the species' distribution (the warmest part of the habitat). Similarly, trailing (warm, equatorward) distributional edges should shift at the

depth-specific velocity of the deep limit of the species' distribution (the coolest part of the available habitat).

Marine biodiversity data. Marine biodiversity maps were extracted from the latest version of AquaMaps⁵⁰. AquaMaps predicts marine species' distributions using a probability of occurrence (0–1) derived from an environmental niche model (for example, explanatory variables including temperature, salinity and oxygen) at 0.5° spatial resolution. It includes 33,518 marine species, 23,700 of which have environmental envelopes generated using at least ten observations—the observation threshold we used here and used by others¹⁴. We followed Klein et al.⁵³ using a minimum threshold of 0.5 probability of occurrence to define range maps for our analysis, which yielded a total of 20,019 species' distribution maps (Supplementary Table 3).

Species' distribution maps were upscaled from their original resolution (0.5°) to 1° to match the resolution of the climate velocities by applying a 50% cell occupancy criterion following García Molinos et al.¹⁴. We categorized species' distributions according to their depth preferences using the same criteria as we used for computing depth-wise climate velocities. This yielded a total of 20,019 species: 16,908 species in the surface layer ($0\text{--}200 \text{ m}$), 2,491 species in the mesopelagic layer ($200\text{--}1,000 \text{ m}$) and 598 species in the bathypelagic layer ($1,000\text{--}4,000 \text{ m}$) (See Supplementary Table 3 for more information about main groups per ocean layer). Because data were sparse in deeper oceans layers, with only 22 species below $4,000 \text{ m}$ (Supplementary Table 3), we analysed biodiversity only in ocean layers above this depth. We assessed the relationship between contemporary climate and biodiversity by correlating the magnitude of climate velocity with the number of species (richness) in each 1° cell.

Marine protected areas and climate velocity trajectories. We downloaded the most up-to-date global dataset on the spatial extents of MPAs from the UNEP-WCMC database (www.protectedplanet.net). To examine how the magnitude and direction of climate velocity in the global MPA network change at different depths in the ocean, we produced climate velocity trajectories³⁶ for the period 2019–2100 from GCMs by forward iteration of isotherms located at the centre of each 0.1° cell within large MPAs ($>100,000 \text{ km}^2$) for two depth layers (surface and mesopelagic) following the direction and speed of local climate velocities^{32,36,50}. All calculations were performed using the VoCC R package⁵⁰.

Caveats. Our study shows results derived from climate models that have several sources of uncertainty. First, uncertainties associated with climate models arise mainly from differences within and among CMIP5 GCMs and among projections for different emission scenarios⁵⁴. These uncertainties might also generate differences in estimates of climate velocity. Second, climate velocity does not have any direct measure of uncertainty³². However, for each depth layer and climate scenario (historical and projection), we estimated standard errors associated with the linear temporal trend component of the local climate velocity (numerator of climate velocity; Extended Data Fig. 6). We noticed that, with depth, standard errors of the temporal trend tend to zero and the pattern becomes similar across climate scenarios. We also estimated the uncertainty of climate velocity among 11 models for the three RCPs and for the historical period by calculating the metric for each individual model. We took the pooled data for each pixel across these 11 new climate velocity estimates and then computed the overall spatial median and interquartile range as a measure of uncertainty in climate velocity associated with the different models. We noticed that this metric of uncertainty increased with depth and with radiative forcing associated with the emission scenarios (Extended Data Fig. 7 and Supplementary Table 4)⁵⁴ making it necessary also to caveat the interpretation that climate velocity is omnidirectional in the deep ocean. These ranges also reflect the decline in data availability with increasing depth in the ocean (Supplementary Table 2) and the sensitivity of climate velocity to its constituent components: the temporal trend and the spatial gradient⁵⁵. However, the fact that the spatial gradient (denominator of the local climate velocity approach) is relatively unaffected by emission scenario across depths does not imply that the temporal trend (numerator of the local climate velocity approach) is a suitable proxy for climate velocity. Because spatial gradients in temperature flatten with depth, a small temperature change through time will propagate rapidly across the thermally homogenous habitat, forcing species to move further and faster to maintain their thermal niches. This is an important consideration, especially for deep-ocean taxa that might lack the vagility of taxa occupying the surface layers of the ocean.

Finally, we used annual mean temperature at different depths as the main environmental driver of the distribution of biodiversity. However, consideration of other aspects of temperature might represent different and relevant biological processes^{56,57}. For example, annual means can be used to infer shifts over the entire species' range but extreme values of temperature (annual minimum and maximum values) can be also used to infer range shifts at the edges of a species' distribution. In addition, monthly data can be used to include seasonal components in climate velocity estimates¹². These aspects were beyond the scope of the current study but could be considered in further research.

Reporting Summary. Further information on research design is available in the Nature Research Reporting Summary linked to this article.

Data availability

Ocean temperature rasters for each depth layer (historical and RCPs scenarios) are available at Zenodo under the identifier <https://doi.org/10.5281/zenodo.3596584>. Correspondence and requests for materials should be addressed to I.B.M.

Code availability

Scripts are available at Zenodo under the identifier <https://doi.org/10.5281/zenodo.3596584>.

References

40. Dobrowski, S. Z. et al. The climate velocity of the contiguous United States during the 20th century. *Glob. Change Biol.* **19**, 241–251 (2013).
41. Dobrowski, S. Z. & Parks, S. A. Climate change velocity underestimates climate change exposure in mountainous regions. *Nat. Commun.* **7**, 12349 (2016).
42. Vrac, M., Stein, M. L., Hayhoe, K. & Liang, X.-Z. A general method for validating statistical downscaling methods under future climate change. *Geophys. Res. Lett.* **34**, L18701 (2007).
43. Rogers, A. D. Environmental change in the deep ocean. *Annu. Rev. Environ. Resour.* **40**, 1–38 (2015).
44. Schulzweida, U. *CDO User Guide v1.9.8* (Zenodo, 2019).
45. R Core Team. *R: A Language and Environment for Statistical Computing* (R Foundation for Statistical Computing, 2018).
46. Tittensor, D. P. et al. Global patterns and predictors of marine biodiversity across taxa. *Nature* **466**, 1098–1101 (2010).
47. Sunday, J. M., Bates, A. E. & Dulvy, N. K. Thermal tolerance and the global redistribution of animals. *Nat. Clim. Change* **2**, 686–690 (2012).
48. Richardson, A. J. In hot water: zooplankton and climate change. *ICES J. Mar. Sci.* **65**, 279–295 (2008).
49. Sen Gupta, A. et al. Episodic and non-uniform shifts of thermal habitats in a warming ocean. *Deep Sea Res. Part II* **113**, 59–72 (2015).
50. García Molinos, J., Schoeman, D. S., Brown, C. J. & Burrows, M. T. VoCC: an R package for calculating the velocity of climate change and related climatic metrics. *Methods Ecol. Evol.* **10**, 2195–2202 (2019).
51. Sunday, J. M. et al. Species traits and climate velocity explain geographic range shifts in an ocean-warming hotspot. *Ecol. Lett.* **18**, 944–953 (2015).
52. Brown, A. & Thatje, S. The effects of changing climate on faunal depth distributions determine winners and losers. *Glob. Change Biol.* **21**, 173–180 (2015).
53. Klein, C. J. et al. Shortfalls in the global protected area network at representing marine biodiversity. *Sci. Rep.* **5**, 17539 (2015).
54. Eyring, V. et al. Taking climate model evaluation to the next level. *Nat. Clim. Change* **9**, 102–110 (2019).
55. Schliep, E. M., Gelfand, A. E. & Clark, J. S. Stochastic modeling for velocity of climate change. *J. Agric. Biol. Environ. Stat.* **20**, 323–342 (2015).
56. Hamann, A., Roberts, D. R., Barber, Q. E., Carroll, C. & Nielsen, S. E. Velocity of climate change algorithms for guiding conservation and management. *Glob. Change Biol.* **21**, 997–1004 (2015).
57. Carroll, C., Lawler, J. J., Roberts, D. R. & Hamann, A. Biotic and climatic velocity identify contrasting areas of vulnerability to climate change. *PLoS ONE* **10**, e0140486 (2015).

Acknowledgements

I.B.M. is supported by the Advanced Human Capital Program of the Chilean National Research and Development Agency (grant no. 72170231). A.J.R. is supported by Australian Government grant no. ARC DP190102293. J.G.M. is funded by the Tenure-Track System Promotion Program of the Japanese Ministry of Education, Culture, Sports, Science and Technology. N.A.D. is supported by the Fundación Bancaria 'la Caixa' Postgraduate Fellowship (LCF/BQ/AA16/11580053). C.J.K. is supported by The University of Queensland Postdoctoral Fellowship.

Author contributions

I.B.M., D.S.S. and A.J.R. conceived the research. K.K., C.G. and K.K.R. provided the marine biodiversity data. I.B.M and D.S.S. analysed the data. I.B.M, D.S.S. and A.J.R. wrote the first draft. I.B.M., D.S.S., A.J.R., J.G.M., M.T.B., N.A.D. and C.J.K. contributed equally to discussion of ideas and analyses. All authors commented on the manuscript.

Competing interests

The authors declare no competing interests.

Additional information

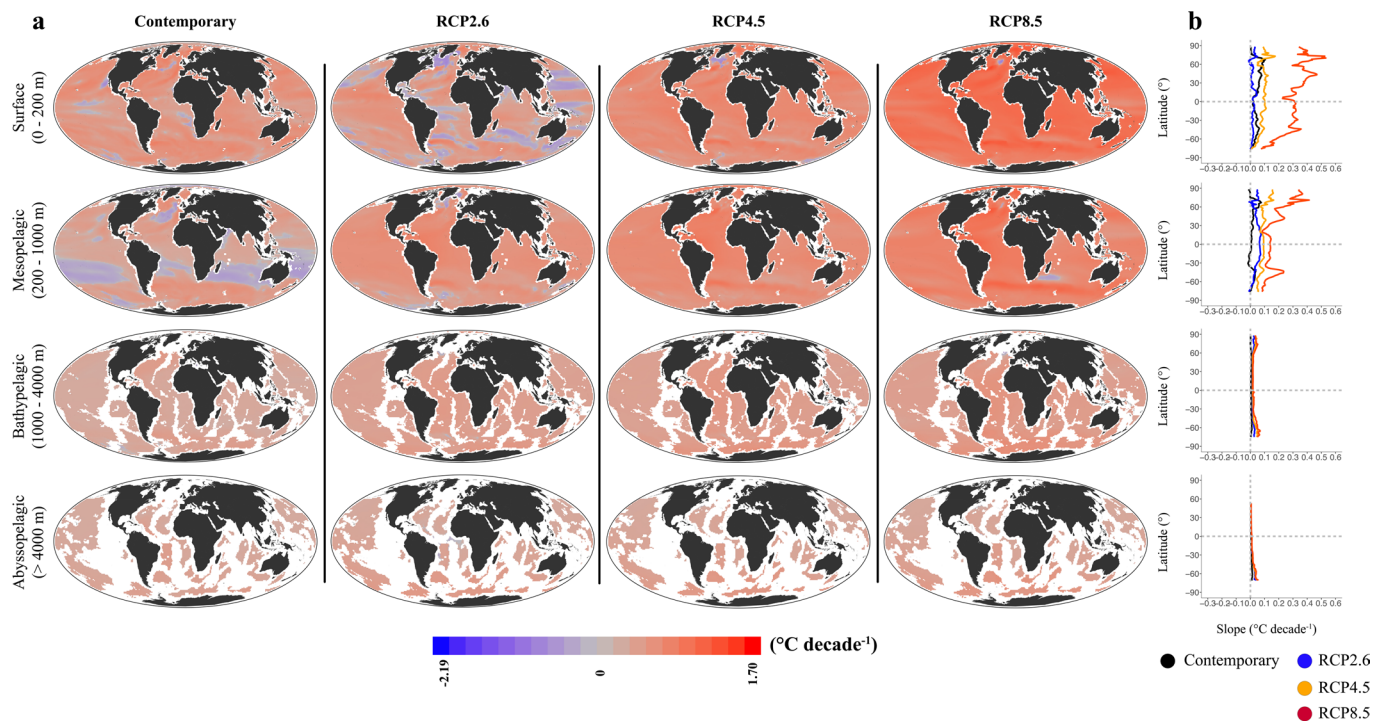
Extended data is available for this paper at <https://doi.org/10.1038/s41558-020-0773-5>.

Supplementary information is available for this paper at <https://doi.org/10.1038/s41558-020-0773-5>.

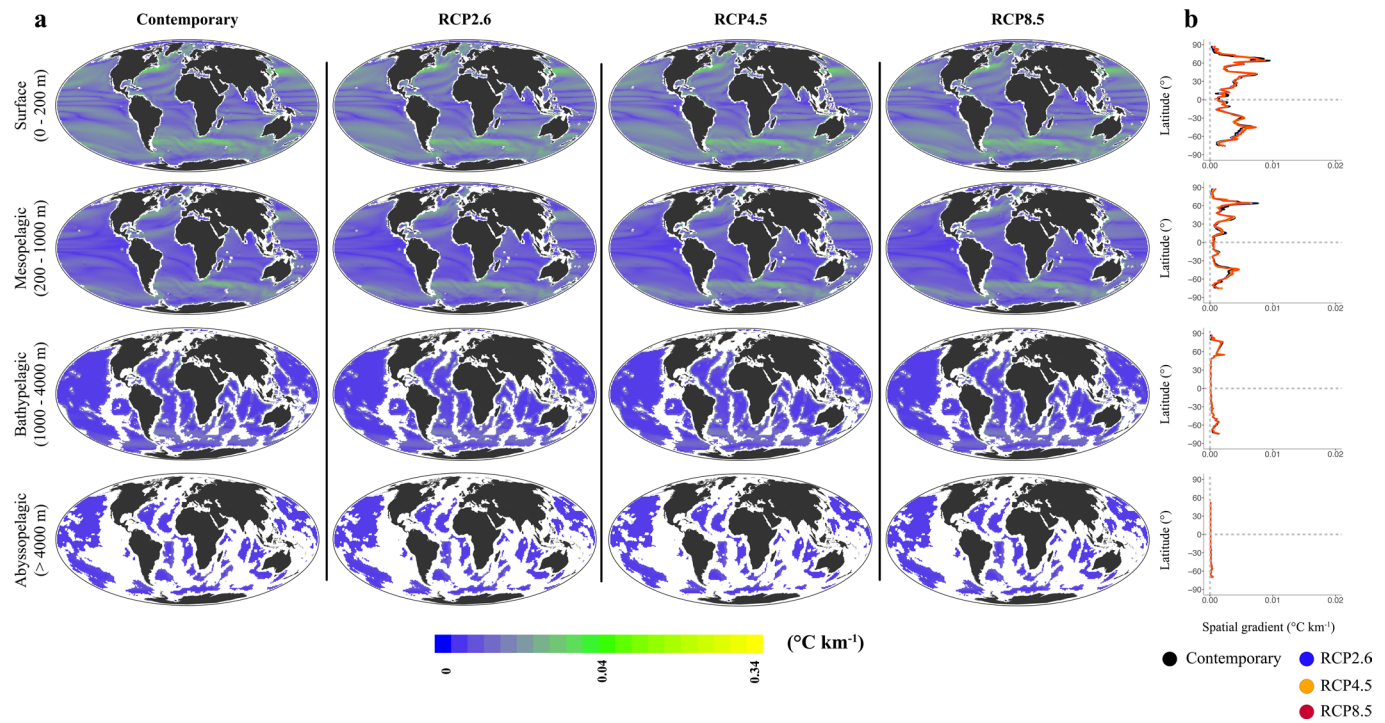
Correspondence and requests for materials should be addressed to I.B.-M.

Peer review information *Nature Climate Change* thanks Conor Walcock and the other, anonymous, reviewer(s) for their contribution to the peer review of this work.

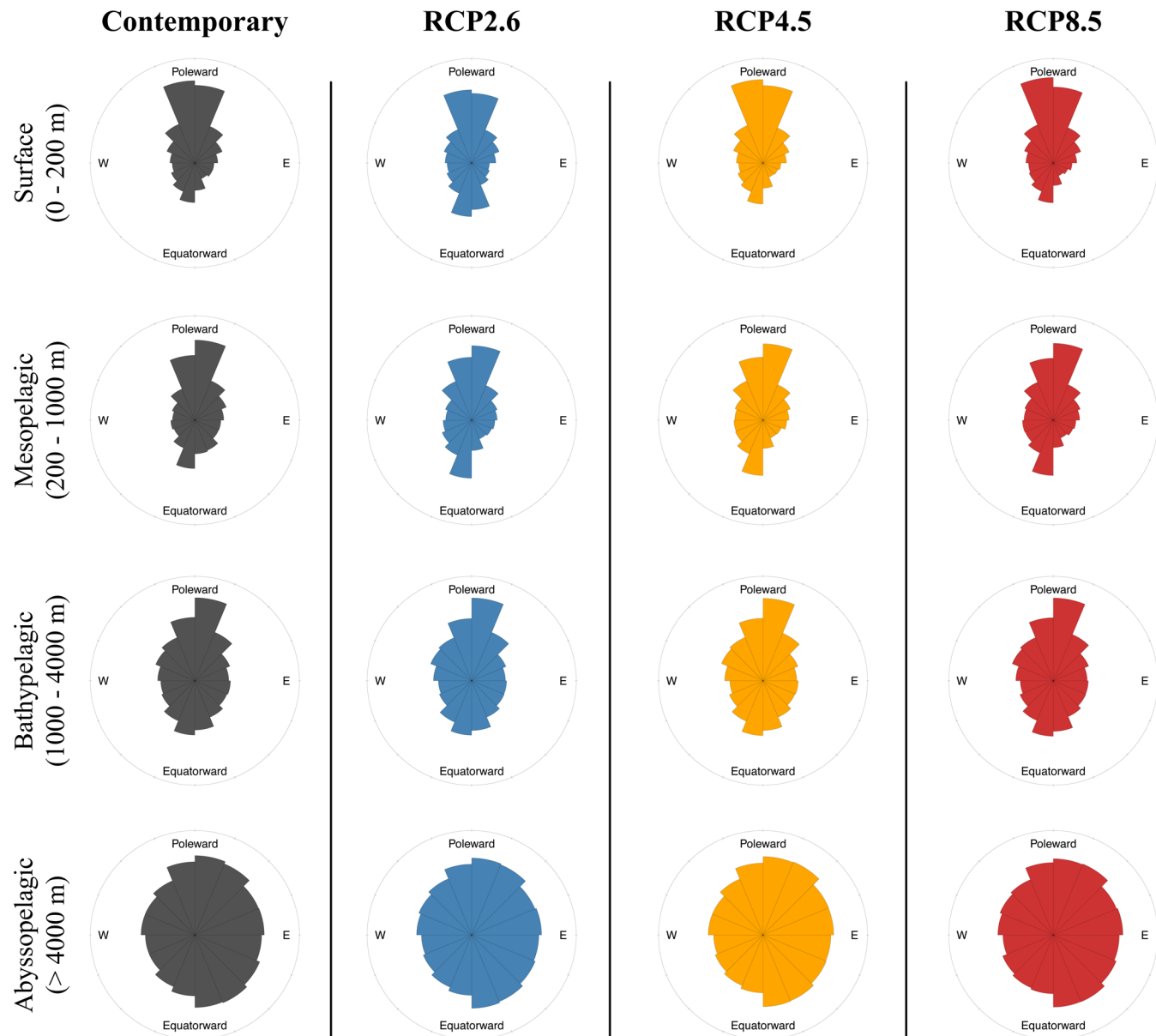
Reprints and permissions information is available at www.nature.com/reprints.



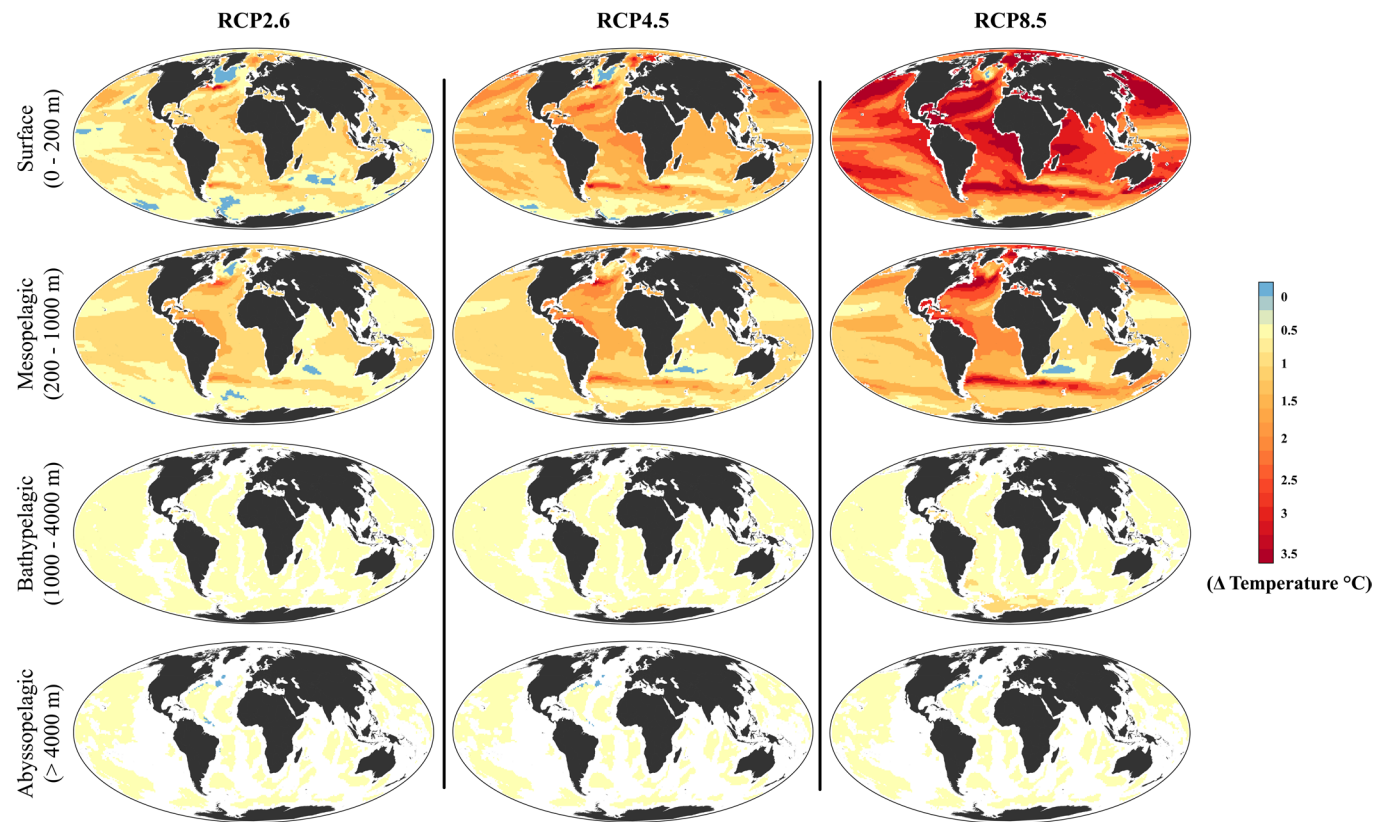
Extended Data Fig. 1 | Temporal trend component of climate velocity. **a**, Temporal trend ($^{\circ}\text{C decade}^{-1}$) for contemporary (1955–2005) and projected sea temperatures (2050–2100) at four different depths in the ocean under three IPCC scenarios (RCP2.6, RCP4.5 and RCP8.5). **b**, Median climate velocity values by 1° of latitude. White bands in deeper layers represent areas where there is no water because of seafloor features extending into pelagic zones.



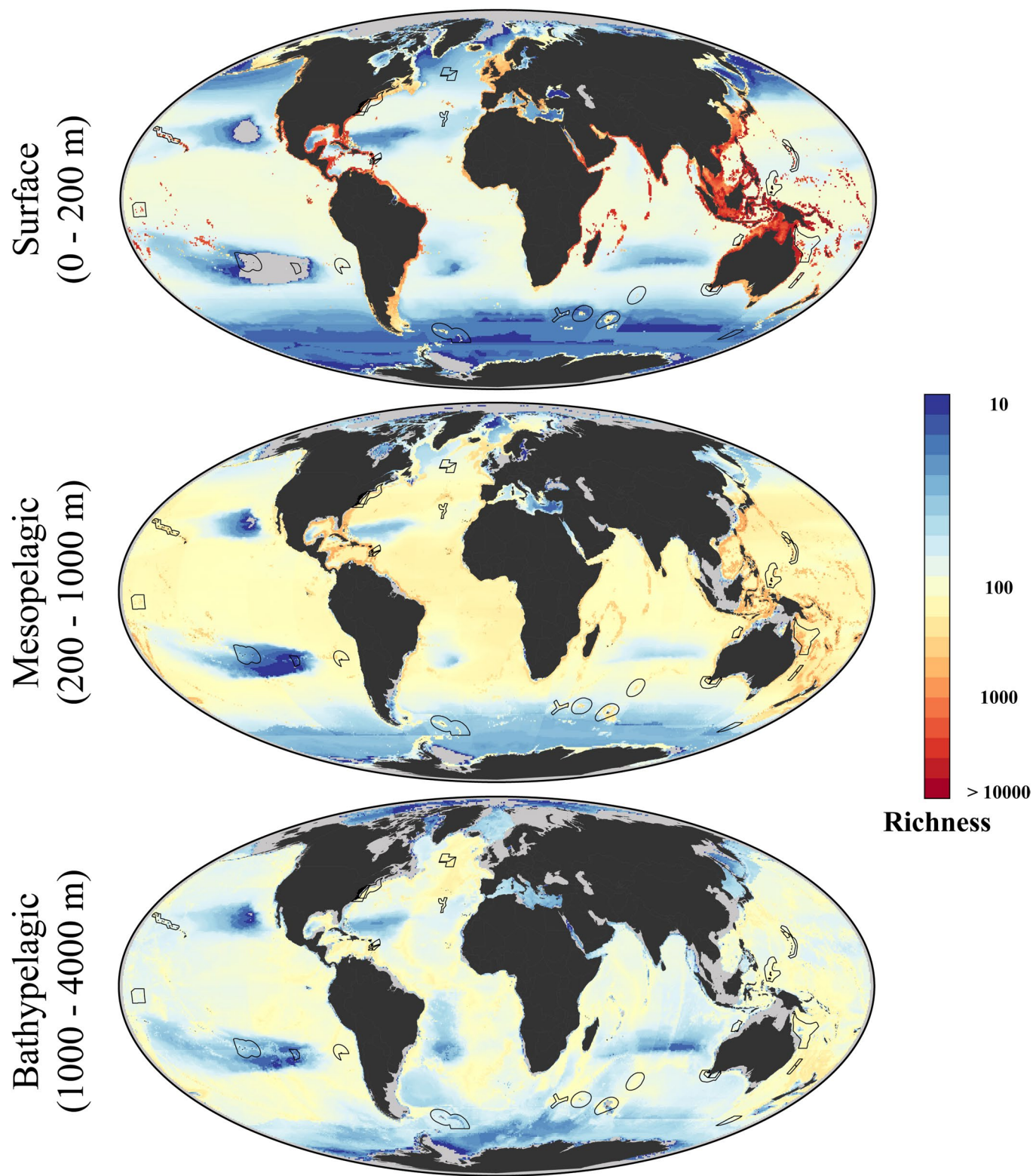
Extended Data Fig. 2 | Spatial gradient component of climate velocity. **a**, Spatial gradient ($^{\circ}\text{C km}^{-1}$) for contemporary (1955–2005) and projected sea temperatures (2050–2100) at four different depths in the ocean under three IPCC scenarios (RCP2.6, RCP4.5 and RCP8.5). **b**, Median climate velocity values by 1° of latitude. White bands in deeper layers represents areas where there is no water because of seafloor features extending into pelagic zones.



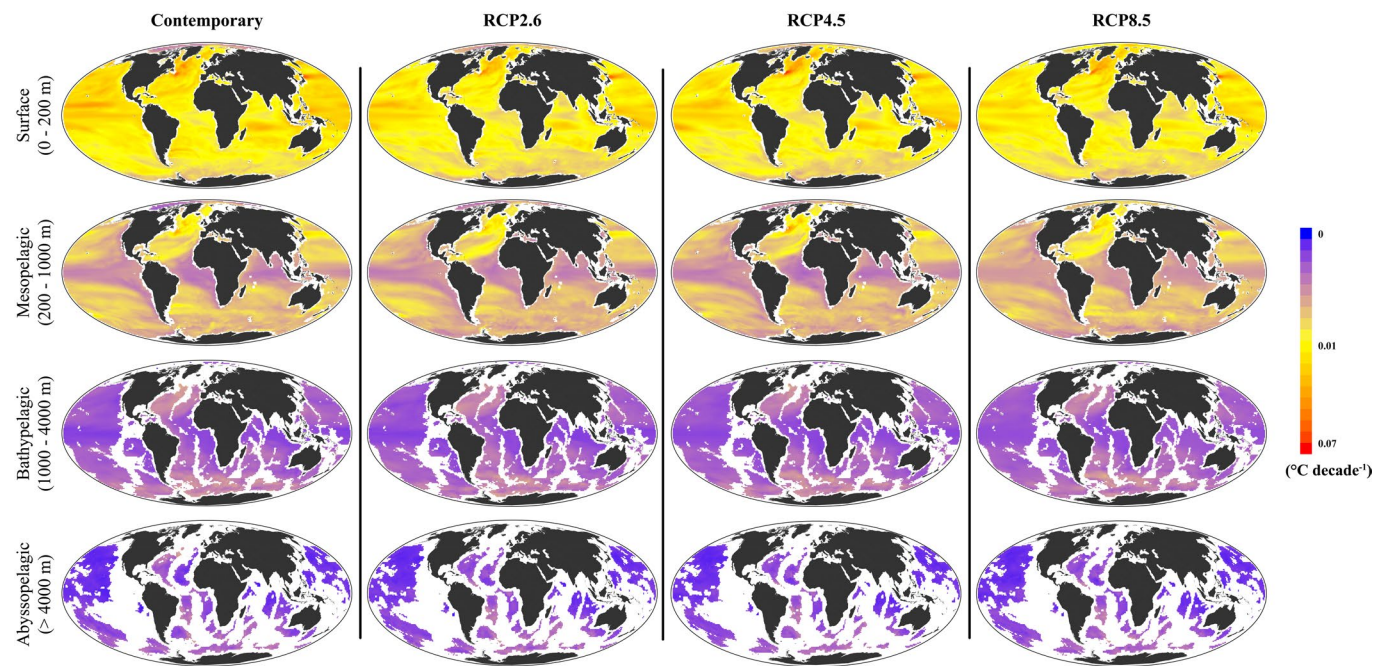
Extended Data Fig. 3 | Direction of climate velocity. Direction of climate velocity for contemporary (1955–2005) and projected future sea temperatures (2050–2100) at four different depths in the ocean under three IPCC scenarios (RCP2.6, RCP4.5 and RCP8.5). Directions standardized by hemisphere to poleward/equatorward directions.



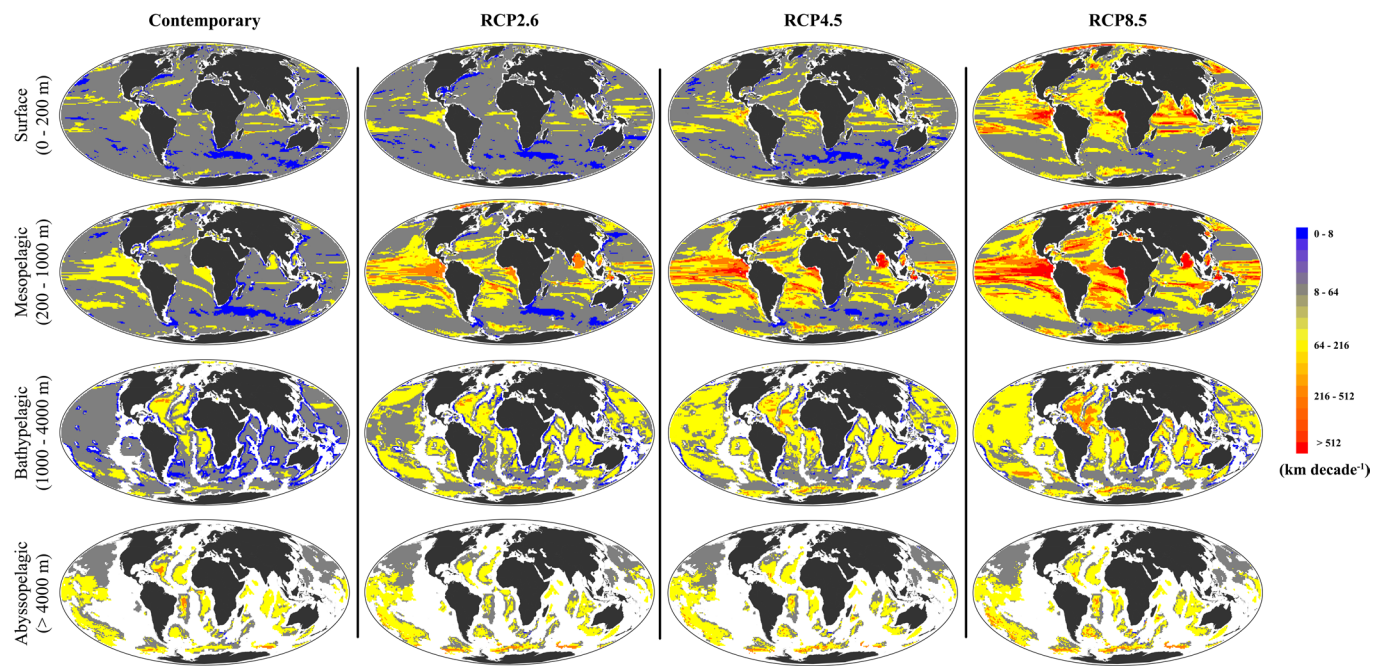
Extended Data Fig. 4 | Global changes in temperature by 2100 relative to 2019. Global changes in temperature conditions at four different layers in the ocean by 2100 relative to present day conditions (2019) under three IPCC scenarios (RCP2.6, RCP4.5 and RCP8.5). White grid squares in deeper layers represent areas where seafloor features extending upward toward the surface mean that there are no sea temperature data available at this depth.



Extended Data Fig. 5 | Species richness for three ocean layers in the ocean. Species richness with a probability of occurrence > 0.5 for three different layers in the ocean. Polygons represent MPAs with areas $> 100,000 \text{ km}^2$ ($n=23$). Grey cells represent missing species richness data for that depth layer, given the threshold for probability of occurrence.



Extended Data Fig. 6 | Standard errors associated to the linear temporal trend component of climate velocity. Standard errors ($^{\circ}\text{C decade}^{-1}$) associated to the linear temporal trend component of climate velocity for contemporary (1955–2005) and projected future sea temperatures (2050–2100) at four different depths in the ocean under three IPCC scenarios (RCP2.6, RCP4.5 and RCP8.5). White grid squares in deeper layers represent areas where seafloor features extending upward toward the surface mean that there are no sea temperature data available at this depth.



Extended Data Fig. 7 | Interquartile range of climate velocity among models. Interquartile range (75th–25th) of climate velocity among models ($n=11$) for contemporary (1955–2005) and projected future sea temperatures (2050–2100) at five different depths in the ocean and under three IPCC scenarios (RCP2.6, RCP4.5 and RCP8.5). White grid squares in deeper layers represent areas where seafloor features extending upward toward the surface mean that there are no sea temperature data available at this depth.

Reporting Summary

Nature Research wishes to improve the reproducibility of the work that we publish. This form provides structure for consistency and transparency in reporting. For further information on Nature Research policies, see [Authors & Referees](#) and the [Editorial Policy Checklist](#).

Statistics

For all statistical analyses, confirm that the following items are present in the figure legend, table legend, main text, or Methods section.

n/a Confirmed

- The exact sample size (n) for each experimental group/condition, given as a discrete number and unit of measurement
- A statement on whether measurements were taken from distinct samples or whether the same sample was measured repeatedly
- The statistical test(s) used AND whether they are one- or two-sided
Only common tests should be described solely by name; describe more complex techniques in the Methods section.
- A description of all covariates tested
- A description of any assumptions or corrections, such as tests of normality and adjustment for multiple comparisons
- A full description of the statistical parameters including central tendency (e.g. means) or other basic estimates (e.g. regression coefficient) AND variation (e.g. standard deviation) or associated estimates of uncertainty (e.g. confidence intervals)
- For null hypothesis testing, the test statistic (e.g. F , t , r) with confidence intervals, effect sizes, degrees of freedom and P value noted
Give P values as exact values whenever suitable.
- For Bayesian analysis, information on the choice of priors and Markov chain Monte Carlo settings
- For hierarchical and complex designs, identification of the appropriate level for tests and full reporting of outcomes
- Estimates of effect sizes (e.g. Cohen's d , Pearson's r), indicating how they were calculated

Our web collection on [statistics for biologists](#) contains articles on many of the points above.

Software and code

Policy information about [availability of computer code](#)

Data collection

Climate models were obtained from the Coupled Model Intercomparison Project Phase 5 (Earth System Grid Federation, <https://esgf-node.llnl.gov/>; Supplementary Table 3). Marine biodiversity data were obtained from the latest version of AquaMaps (Kaschner et al. 2019; Supplementary Table 4)

Data analysis

We used CDO (climate data operators) and R 3.5.0 to analyze the data in this study. Codes and Scripts are available at GitHub repository archived at Zenodo <http://doi.org/10.5281/zenodo.3596584>

For manuscripts utilizing custom algorithms or software that are central to the research but not yet described in published literature, software must be made available to editors/reviewers. We strongly encourage code deposition in a community repository (e.g. GitHub). See the Nature Research [guidelines for submitting code & software](#) for further information.

Data

Policy information about [availability of data](#)

All manuscripts must include a [data availability statement](#). This statement should provide the following information, where applicable:

- Accession codes, unique identifiers, or web links for publicly available datasets
- A list of figures that have associated raw data
- A description of any restrictions on data availability

Data used in this study can be found in GitHub under Zenodo identifier <http://doi.org/10.5281/zenodo.3596584>

Field-specific reporting

Please select the one below that is the best fit for your research. If you are not sure, read the appropriate sections before making your selection.

- Life sciences Behavioural & social sciences Ecological, evolutionary & environmental sciences

For a reference copy of the document with all sections, see nature.com/documents/nr-reporting-summary-flat.pdf

Life sciences study design

All studies must disclose on these points even when the disclosure is negative.

Sample size	We used 11 CMIP5 climate models under historical (hist) and future scenarios (RCPs: 2.6, 4.5, 8.5).
Data exclusions	We excluded climate models that did not have the four scenarios previously mentioned to keep consistency among models. We also exclude from our analysis coastal marine protected areas (MPAs) and we focused on open-ocean MPAs with areas > 100,000 km ² .
Replication	This study does not include any experimental design.
Randomization	This study does not include any level of randomization.
Blinding	The data were collected from Earth System Grid Federation and models can be traced back to its original source.

Reporting for specific materials, systems and methods

We require information from authors about some types of materials, experimental systems and methods used in many studies. Here, indicate whether each material, system or method listed is relevant to your study. If you are not sure if a list item applies to your research, read the appropriate section before selecting a response.

Materials & experimental systems

n/a	Involved in the study
<input checked="" type="checkbox"/>	Antibodies
<input checked="" type="checkbox"/>	Eukaryotic cell lines
<input checked="" type="checkbox"/>	Palaeontology
<input checked="" type="checkbox"/>	Animals and other organisms
<input checked="" type="checkbox"/>	Human research participants
<input checked="" type="checkbox"/>	Clinical data

Methods

n/a	Involved in the study
<input checked="" type="checkbox"/>	ChIP-seq
<input checked="" type="checkbox"/>	Flow cytometry
<input checked="" type="checkbox"/>	MRI-based neuroimaging